Hindawi Publishing Corporation
Bioinorganic Chemistry and Applications
Volume 2010, Article ID 149149, 11 pages
doi:10.1155/2010/149149

Research Article

Antineoplastic Activity of New Transition Metal Complexes of 6-Methylpyridine-2-carbaldehyde-N(4)-ethylthiosemicarbazone: X-Ray Crystal Structures of [VO_2(mpETSC)] and [Pt(mpETSC)Cl]

Shadia A. Elsayed,[1] Ahmed M. El-Hendawy,[2] Sahar I. Mostafa,[3] Bertrand J. Jean-Claude,[4] Margarita Todorova,[4] and Ian S. Butler[1]

[1] *Department of Chemistry, McGill University, Montreal, QC, Canada H3A 2K6*
[2] *Chemistry Department, Faculty of Science, Mansoura University, Damietta 34517, Egypt*
[3] *Chemistry Department, Faculty of Science, Mansoura University, Mansoura, Egypt*
[4] *Department of Medicine, Royal Victoria Hospital, Montreal, QC, Canada H3A 1A1*

Correspondence should be addressed to Ian S. Butler, ian.butler@mcgill.ca

Received 14 March 2010; Accepted 14 April 2010

Academic Editor: Spyros Perlepes

New complexes of dioxovanadium(V), zinc(II), ruthenium(II), palladium(II), and platinum(II) with 6-methylpyridine-2-carbaldehyde-N(4)-ethylthiosemicarbazone (HmpETSC) have been synthesized. The composition of these complexes is discussed on the basis of elemental analyses, IR, Raman, NMR (^{1}H, ^{13}C, and ^{31}P), and electronic spectral data. The X-ray crystal structures of [VO_2(mpETSC)] and [Pt(mpETSC)Cl] are also reported. The HmpETSC and its [Zn(HmpETSC)Cl_2] and [Pd(mpETSC)Cl] complexes exhibit antineoplastic activity against colon cancer human cell lines (HCT 116).

1. Introduction

Interest in thiosemicarbazone chemistry has flourished for many years, largely as a result of its wide range of uses, for example, as antibacterial, antifungal, chemotherapeutic, and bioanalytical agents [1–6]. One particular area of thiosemicarbazone chemistry that has been increasing in importance recently involves biologically active metal complexes of thiosemicarbazone-based chelating (NNS) agents. As the coordination of the metal ions to thiosemicarbazones improves their efficacy and improve their bioactivity [6]. In this concept, zinc(II), palladium(II), and platinum(II) complexes of pyridine-2-carboxaldehyde thiosemicarbazone and substituted pyridine thiosemicarbazone were tested against human cancer breast and bladder cell lines and found to be selectively cytotoxic to these malignant cell carcinoma [7, 8]. We have previously studied the chemotherapeutic potential of a series of Mo(VI), Pd(II), Pt(II), and Ag(I) complexes with N,O; N,S and O,O-donors. These complexes were found to display significant anticancer activity against *Ehrlich ascites tumor cell* (EAC) in albino mice [9–12]. Copper(II) complexes of 6-methylpyridine-2-carbaldehyde and its N(4)-methyl, ethyl, and phenyl thiosemicarbazones have been reported as well as their activity against pathogenic fungi [13]. In this paper, we report the synthesis and spectroscopic characterizations of new complexes of 6-methylpyridine-2-carbaldehyde-N(4)-ethylthiosemicarbazone (HmpETSC, Figure 1) with V(V), Zn(II), Ru(II), Pd(II), and Pt(II). The X-ray crystal structures of [VO_2(mpETSC)] and [Pt(mpETSC)Cl] have been reported. Also, the anticancer activity of HmpETSC and its Zn(II) and Pd(II) complexes toward colon cancer human cell lines has been tested.

2. Experimental

All reagents were purchased from Alfa/Aesar and Aldrich. [$RuCl_2(PPh_3)_3$] was prepared as previously reported in [14]. Infrared spectra were recorded using a Nicolet 6700 Diamond ATR spectrometer in the 200–4000 cm^{-1} range. Raman spectra were recorded on in Via Renishaw

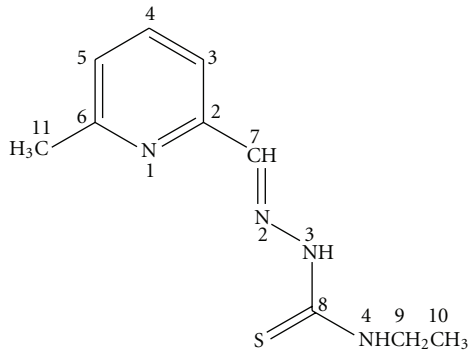

Figure 1: Structure of 6-methylpyridine-2-carbaldehyde-N(4)-ethylthiosemicarbazone (HmpETSC).

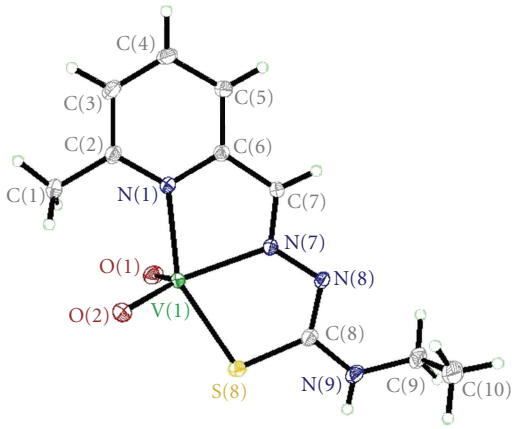

Figure 2: Structure of $[VO_2(mpETSC)]$ with numbering scheme.

spectrometer using 785 nm laser excitation. NMR spectra were recorded on Varian Mercury 500 MHz spectrometer in DMSO-d6 with TMS as reference. Electronic spectra were recorded in DMF using Hewlett-Packard 8453 Spectrophotometer. Elemental analyses and X-ray crystallography were performed in Université De Montréal. The human cancer cell lines were obtained from the American Type Culture Collection (ATCC catalog number): HCT116 human colorectal carcinoma (CCL-247). Cells were maintained in Roswell Park Memorial Institute (RPMI-1640) medium (Wisent Inc., St-Bruno, Canada) supplemented with 10% FBS, 10 mM HEPES, 2 mM L-gutamine, and 100 μg/mL penicillin/streptomycin (GibcoBRL, Gaithersburg, MD). All assay cells were plated 24 hours before drug treatment.

2.1. Preparation of the Ligand: 6-Methylpyridine-2-carboxaldehyde-N(4)-ethylthiosemicarbazone (HmpETSC). 6-Methylpyridine-2-carboxaldehyde (1.21 g, 10 mmol) in ethanol (10 cm^3) was added to N(4)-ethylthiosemicarbazide (1.19 g, 10 mmol) in ethanol-water solution (V/V 1 : 1, 80 cm^3) followed by the addition of drops of glacial acetic acid. The reaction mixture was refluxed for 3 hours. The precipitate obtained was filtered off, washed with water and ethanol, and recrystallized from ethanol then dried in vacuo. m. p. = 201°C. Elemental analytical calculation for $C_{10}H_{13}N_4S$: C, 54.0, H, 6.4; N, 25.2; S, 14.4% found C, 54.0, H, 6.3; N, 25.1; S, 14.2%.

2.2. Preparation of the Complexes

2.2.1. $[VO_2(mpETSC)]$. To a solution of HmpETSC (0.044 g, 0.2 mmol) in acetonitrile (10 cm^3), $[VO(acac)_2]$ (0.053 g, 0.2 mmol) was added. The reaction mixture was refluxed for 1 hour. Upon cooling the yellowish green solution, orange precipitate was obtained. It was filtered off, washed with ethanol, and dried in vacuo. The brown crystals suitable for X-Ray crystallography were obtained by a slow evaporation of a solution of the complex in acetonitrile. The yield was 50% (based on the metal). Elemental analytical calculation for $C_{10}H_{13}N_4O_2SV$: C, 39.5; H, 4.3; N, 18.4; S, 10.5% found C, 39.4; H, 4.0; N, 18.2; S, 10.3%.

2.2.2. $[Zn(HmpETSC)Cl_2]$. A methanolic solution (10 cm^3) of HmpETSC (0.044 g, 0.2 mmol) was added to $ZnCl_2$ (0.027 g, 0.2 mmol) in methanol (10 cm^3). The reaction mixture was refluxed for 2 hours, and the off-white product obtained was filtered off, washed with methanol, then dried in air. The yield was 35% (based on the metal). Elemental analytical calculation for $C_{10}H_{14}Cl_2N_4SZn$: C, 33.5; H, 3.9; N, 15.6; S, 8.9% found C, 33.7; H, 3.7; N, 15.5; S, 8.8%.

2.2.3. $[Ru(PPh_3)_2(mpETSC)_2]$. A hot ethanolic solution of HmpETSC (0.044 g, 0.2 mmol) was added to $[RuCl_2(PPh_3)_3]$ (0.1 g, 0.1 mmol). Et_3N (0.02 cm^3, 0.2 mmol) was then added and the reaction mixture was refluxed for 2 hours. The red brown solution was filtered and upon reducing the volume by evaporation a brown solid was isolated. It was filtered off, washed with ethanol and ether. The yield was 33% (based on the metal). Elemental analytical calculation for $C_{56}H_{56}N_8P_2RuS_2$: C, 63.0; H, 5.3; N, 10.5; S, 6.0% found that C, 62.8; H, 5.1; N, 10.4; S, 5.8%.

2.2.4. $[Pd(mpETSC)Cl]$. A solution of $K_2[PdCl_2]$ (0.1 g, 0.3 mmol) in water (2 cm^3) was added to HmpETSC (0.066 g, 0.3 mmol) in methanolic solution of KOH (0.018 g, 0.3 mmol; 15 cm^3). The reaction mixture was stirred at room temperature for 24 hours. The orange precipitate was filtered off, washed with water methanol, and finally air-dried. Yield was 60% (based on metal). Elemental analytical calculation for $C_{10}H_{13}ClN_4PdS$: C, 33.1; H, 3.6; N, 15.4; S, 8.8% found C, 33.4; H, 3.2; N, 15.2; S, 8.5%.

2.2.5. $[Pt(mpETSC)Cl]$. An aqueous solution (3 cm^3) of K_2PtCl_4 (0.042 g, 0.1 mmol) was added dropwise to a methanolic solution of HmpETSC (0.022 g, 0.1 mmol; 15 cm^3). The reaction mixture was stirred overnight at room temperature. Upon evaporation of the solvent, fine red crystals were observed. These were suitable for single crystal X-ray crystallography. Yield was 25% (based on metal). Elemental analytical calculation for $C_{10}H_{13}ClN_4PtS$: C, 26.6;

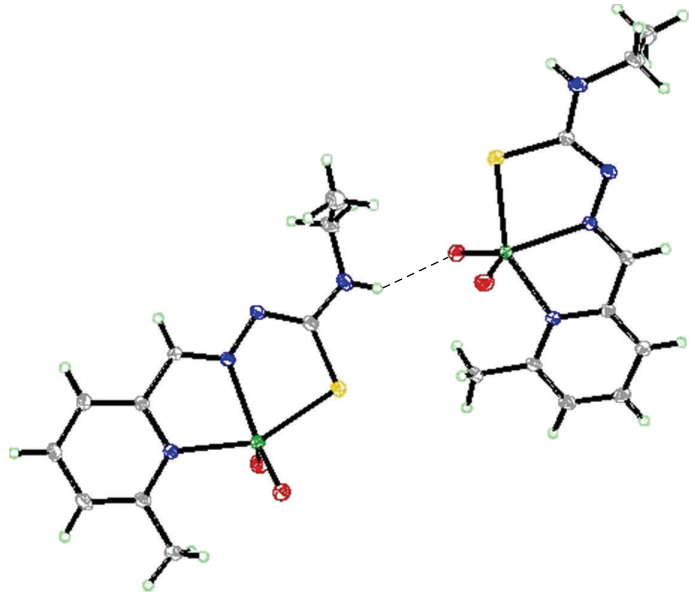

Figure 3: Hydrogen bonding interaction in the lattice of $[VO_2(mpETSC)]$.

H, 2.9; N, 12.4; S, 7.1% found C, 26.8; H, 2.8; N, 12.1; S, 6.9%.

2.3. X-Ray Crystallography. The crystal structure were measured on The X-Ray Crystal Structure Unit, using a Bruker Platform diffractometer, equipped with a Bruker MART 4 K Charger-Coupled Device (CCD) Area Detector using the program APEX II and a Nonius Fr591 rotating anode (Copper radiation) equipped with Montel 200 optics. The crystal-to-detector distance was 5 cm, and the data collection was carried out in 512 × 512 pixel mode. The initial unit cell parameters were determined by the least-squares fit of the angular setting of strong reflections, collected by a 10.0 degree scan in 33 frames over three different parts of the reciprocal space (99 frames total). One complete sphere of data was collected.

The crystals of $[VO_2(mpETSC)]$ and $[Pt(mpETSC)Cl]$ were mounted on the diffractometer, and the unit cell dimensions and intensity data were measured at 200 K. The structures were solved by the least-squares fit of the angular setting of strong reflections based on F^2. The relevant crystal data and experimental conditions along with the final parameters are reported in Table 1.

2.4. Antineoplastic Testing. In the growth inhibition assay, HCT116 cells were plated at 5,000 cells/well in 96-well flat-bottomed microtiter plates (Costar, Corning, NY). After 24-hour incubation, cells were exposed to different concentrations of each compound continuously for four days. Briefly, following HmpETSC and its Zn(II) and Pd(II) complexes treatment, cells were fixed using 50 μl of cold trichloroacetic acid (50%) for 60 minutes at 4°C, washed with water, stained with 0.4% sulforhodamine B (SRB) for 4 hours at room temperature, rinsed with 1% acetic acid, and allowed to dry overnight [15]. The resulting colored residue was dissolved in 200 μl Tris base (10 mM, pH 10.0), and optical density was recorded at 490 nm using a microplate reader ELx808 (BioTek Instruments). The results were analyzed by Graph Pad Prism (Graph Pad Software, Inc., San Diego, CA), and the sigmoidal dose response curve was used to determine 50% cell growth inhibitory concentration (IC_{50}). Each point represents the average of two independent experiments performed in triplicate.

3. Results and Discussion

3.1. Synthesis and Physical Properties of the Complexes. The preparative reactions for the complexes can be represented by the following equations:

$$VO(acac)_2 + HmpETSC \xrightarrow{CH_3CN,T} [VO_2(mpETSC)]$$

$$ZnCl_2 + HmpETSC \xrightarrow{MeOH,T} [Zn(HmpETSC)Cl_2]$$

$$[Ru(PPh_3)_3Cl_2] + HmpETSC \xrightarrow{EtOH/Et_3N,T} [Ru(PPh_3)_2(mpETSC)_2]$$

$$K_2PdCl_4 + HmpETSC \xrightarrow{H_2O/MeOH,T} [Pd(mpETSC)Cl]$$

$$K_2PtCl_4 + HmpETSC \xrightarrow{H_2O/MeOH,T} [Pt(mpETSC)Cl]$$

All the complexes are microcrystalline or amorphous powder, stable in the normal laboratory atmosphere, and slightly soluble in common organic solvent but completely soluble in DMF and DMSO.

Table 1: Crystal data and structure refinement for VO_2(mpETSC) and Pt(mpETSC)Cl.

	[VO_2(mpETSC)]	[Pt(mpETSC)Cl]
Empirical formula	$C_{10}H_{13}N_4\ O_2SV$	$C_{10}H_{13}ClN_4PtS$
Formula weight	304.24	451.84
Temperature	200 K	150 K
Wavelength	1.54178 Å	1.54178 Å
Crystal system	Monoclinic	Monoclinic
Space group	P21/c	P21/n
Unit cell dimensions		
a(Å), α (°)	8.5583(2), 90^o	12.9824(2), 90
b(Å), β (°)	13.4934(3), 03.679(1)^o	b = 7.0655(1). 94.454(1)^0
c(Å), γ (°)	11.2697(3), 90^o	c = 13.6601(2), 90
Volume (Å^3)	1264.52(5) (Å^3)	1249.22(3) (Å^3)
Z, Density (calculated) g/cm^3	4; 1.598 g/cm^3	4; 2.402 g/cm^3
Absorption coefficient	8.122 mm^{-1}	24.402 mm^{-1}
F(000)	624	848
Crystal size	0.26 × 0.10 × 0.06 mm	0.12 × 0.08 × 0.02 mm
Theta range for data collection (°)	5.20 to 72.30°	4.53 to 72.13
Index ranges	$-10 \le h \le 10, -16 \le h \le 16, -13 \le l \le 13$	$-15 \le h \le 15, -8 \le k \le 8, -16 \le l \le 16$
Reflections collected	16371	15858
Independent reflections	2468 [R_{int} = 0.033]	2442 [R_{int} = 0.045]
Absorption correction	Semi-empirical from equivalents	Semi-empirical from equivalents
Max. and min. transmission	0.6143 and 0.3013	0.6138 and 0.3359
Refinement method	Full-matrix least-squares on F^2	Full-matrix least-squares on F^2
Data/restraints/parameters	2468/0/169	2442/0/157
Goodness-of-fit on F^2	1.150	1.065
Final R indices [I>2sigma(I)]	R_1 = 0.0318, wR_2 = 0.0881	R_1 = 0.0277, wR_2 = 0.0951
R indices (all data)	R_1 = 0.0326, wR_2 = 0.0887	R_1 = 0.0307, wR_2 = 0.0993
Extinction coefficient		0.00036(6)
Largest diff. peak and hole	0.414 and −0.711 e/Å^3	1.579 and −1.242 e/Å^3

Table 2: Infrared and Raman spectral data of HmpETSC and its complexes[a].

Compound	ν(NH)	ν(HC=N)	ν(C=C)	ν(N=CS)	ν(N–N)	ν(CS)	ν(M– N)	ν(M–S)	ν(M–Cl)
HmpETSC	3267	1589	1530	—	992	812	—	—	—
		1607	**1579**		**1006**	**824**			
[VO_2(mpETSC)]	3214	1652	1613	1576	1017	787	427		926[b]
		1651	**1570**	**1586**	**1019**	**754**	**427**	**343**	937[b]
[Zn(HmpETSC)Cl_2]	3290	1625	1596		1009	805	466		
		1626	**1598**		**1009**	**793**	**427**	**317**	**300**
[Ru(PPh_3)$_2$(mpETSC)$_2$]	3383	1572	1528	1479	999	788	465		
[Pd(mpETSC)Cl]	3286	1608	1582	1572	1008	784	454		
		1617	**1580**	**1570**	**1022**	**787**	**462**	**345**	**297**
[Pt(mpETSC)Cl]	3322	1607	1580	1570sh	1020	779	424		
		1609	**1584**	**1564**	**1009**	**779**	**421**	**330**	**306**

[a]Raman data are in *bolds*, [b]ν(O=V=O) sym and asym.

3.2. Infrared and Raman Spectra. The infrared and Raman spectral assignments of the ligand, HmpETSC, and its reported complexes are listed in Table 2. HmpETSC has the characteristic thioamide moiety (-HN-C(S)NHEt), which can be present in either thione or thiol form (Figure 1) [16, 17]. The IR and Raman spectra of HmpETSC show the absence of absorption band in 2500–2600 cm^{-1} region indicating the presence of the free HmpETSC in thione form [18]. HmpETSC shows a strong IR band at 1589 cm^{-1}, observed at 1607 cm^{-1} in the Raman, which is corresponding to the azomethine, ν(HC=N), group [13, 19]. In the spectra of the complexes, the shift of this band to higher frequency

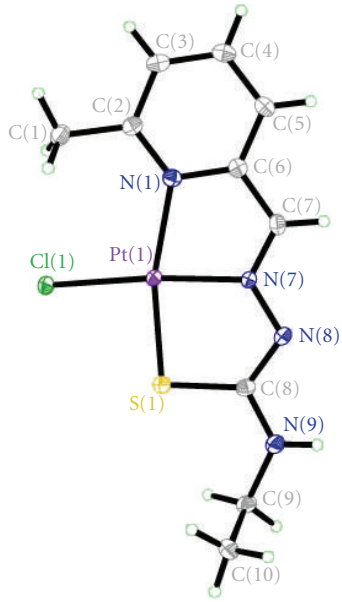

Figure 4: Structure of [Pt(mpETSC)Cl] with numbering scheme.

is observed, suggesting the participation of azomethine nitrogen in the coordination to metal ions [20, 21]. This feature is further supported by the shift of ν(N-N) band in the free ligand (at 992 and 1006 cm^{-1} in IR and Raman, respectively) to higher frequencies upon complexation [18, 22]. On the other hand, the participation of the deprotonated thiol sulfur in coordination was indicated by the shift of the IR band at 812 cm^{-1} (at 824cm^{-1} in the Raman) in the free ligand to lower frequencies in the complexes [19, 23]. This view is supported by the absence of ν(N(3)H) vibration with the observation of new band near 1570 cm^{-1} in the complexes which may assign to ν(N(3)=C) [24]. Furthermore, the coordination of pyridine nitrogen atom is indicated through the positive shift of the ring deformation band in HmpETSC near 582 and 586 cm^{-1} in the IR and Raman spectra, respectively [25]. Both IR and Raman spectral data suggest mononegative tridentate (N, N, S^-) behavior of $mpETSC^-$. In case of [Zn(HmpETSC)Cl_2], the ν(N(3)H) band is observed at lower wave number as the thione sulfur participates in coordination [26]. Also, there is no shift observed in the pyridine ring deformation mode, that is, HmpETSC acts as a neutral bidentate ligand through both thione sulfur and azomethine nitrogen atoms [25].

The spectra of the complexes show that new bands in the IR and Raman near 450 cm^{-1}may assign to ν(M-N) [27]. Also, the far IR and Raman spectra show new bands near 325 and 300 cm^{-1} can be assigned to ν(M-S) and ν(M-Cl), respectively [9, 10].

In the 940–920 cm^{-1} region the IR spectrum of the complex [VO_2(mpETSC)] shows two strong bands characteristic of the *cis*-VO_2 moiety [28, 29].

The presence of the coordinated PPh_3 in the complex [$Ru(PPh_3)_2(mpETSC)_2$] is confirmed by the appearance of the characteristic ν(P-C_{ph}) and δ(C-CH) band at 1085 and 720 cm^{-1}, respectively [30].

3.3. NMR Spectra. Table 3 shows the ^{1}H-NMR spectral data of HmpETSC and its reported complexes in DMSO-d_6 (see Figure 1 for numbering scheme) which are in a great agreement with those reported in the literature [13, 31, 32]. In the spectrum of free HmpETSC, the singlet observed at δ 11.62 ppm assigned to N(3)H is disappeared in the spectra of the complexes indicating that the coordination takes place through the deprotonated thiol sulfur atom [33]. In [Zn(HmpETSC)Cl_2], this band is observed at δ 11.63 ppm, confirming the data observed in the IR and Raman spectra that the coordination of HmpETSC to Zn(II) occurs through the thione sulfur atom [34]. As expected. the singlet observed at δ 8.02 ppm in the free ligand assigned to the azomethine H(7)C=N proton shows downfield shift in the complexes (δ 8.22–8.71 ppm), due to the involvement of azomethine nitrogen in coordination [16, 33]. The spectrum of HmpETSC shows singlet at δ 8.66 ppm assigned to the thioamide N(4)H proton, this signal is shifted upfield upon complexation [32, 34]. This feature may be due to the sequence of establishment of hydrogen bonds formation [35, 36]. The spectrum of HmpETSC exhibits triplet and quartiplet signals at δ1.14 and 3.58 ppm assigned to H(10) and H(9), respectively. Also, the pyridine protons appear in δ 7.22–8.059 ppm region [33]. As expected, these protons are shifted downfield complexes (except in case of [Zn(HmpETSC)Cl_2]) due to the decrease in the electron density caused by electron withdrawal by the metal ions from the sulfur, azomethine nitrogen, and pyridine nitrogen atoms.

^{13}C-NMR assignments of the HmpETSC and its complexes are listed in Table 4 and are in agreement with the reported data [13]. The spectrum of the free ligand shows number of resonances at δ 14.98, 24.49, 38.81, 117.69, 123.78, 137.14, 142.74, 153.18, 158.28, and 177.28 ppm, assigned to C(10), C(11), C(9), C(5), C(3), C(4), C(7), C(6), C(2), and C(8), respectively. In the complexes, the resonances of the carbon atoms adjacent to the coordination sites (C(7), C(8), C(2), and C(6)) are shifted downfield relatively to their positions in the free ligand [37, 38]. This feature may be due to an increase in current brought about by coordination to azomethine nitrogen, pyridine nitrogen, and deprotonated thiol sulfur atoms [25, 39]. In the spectrum of [Zn(HmpETSC)Cl_2] complex, the resonances arising from C(6), C(2) are more or less in the same positions as in the free ligand indicating that HmpETSC acts as a neutral bidentate ligand through thione sulfur and azomethine nitrogen atoms [25].

The ^{31}P-NMR spectrum of [$Ru(PPh_3)_2(mpETSC)_2$] shows a sharp singlet at δ 52.48 ppm, suggesting the presence of the two PPh_3 groups in *trans*-configuration [30].

3.4. Electronic Spectra. The electronic spectrum of HmpETSC shows bands at 340 and 300 nm assigned to $\pi \rightarrow \pi^*$ and $n \rightarrow \pi^*$ of the azomethine and pyridine ring transitions, respectively [40, 41]. In the complexes, both transitions undergo blue shifts indicating the coordination *via* the azomethine and pyridine nitrogen atoms [42].

The electronic spectra of [M(mpETSC)Cl] (M(II) = Pd, Pt) show that two bands near 475 and 330 nm can be assigned

Figure 5: Hydrogen bonding interaction in the lattice of [Pt(mpETSC)Cl].

Table 3: ^{1}H-NMR spectral data of HmpETSC and its complexes.

Compound	H(3) (d)	H(4) (t)	H(5) (d)	H(7)CH=N (s)	H(9) (q)	H(10) (t)	Me(py) (s)	N(3)H (s)	N(4)H (s)
HmpETSC	8.06	7.71	7.22	8.02	3.58	1.14	2.45	11.62	8.67
$[VO_2(mpETSC)]$	7.56	8.11	7.67	8.58	3.32	1.12	2.48	—	8.19
$[Zn(HmpETSC)Cl_2]$	8.02	7.73	7.23	8.71	3.58	1.13	2.46	11.63	8.67
$[Ru(PPh_3)_2(mpETSC)_2]$	7.55	7.45	7.38	8.63	3.34	0.88	2.38	—	—[a]
[Pd(mpETSC)Cl]	7.55	7.95	7.38	8.22	3.23	1.07	2.49	—	7.95
[Pt(mpETSC)Cl]	7.55	8.55	7.46	8.22	3.31	1.08	2.48	—	7.98

[a] Overlapped with Ph protons.

Table 4: ^{13}C-NMR spectral data of HmpETSC and its complexes.

Compound	C(2)	C(3)	C(4)	C(5)	C(6)	C(HC=N)	(C(C=S))	C(9)	C(10)	C(11)
HmpETSC	158.28	123.78	137.14	117.69	153.18	142.74	177.28	38.81	14.98	24.49
$[VO_2(mpETSC)]$	163.16	127.39	142.76	123.26	153.75	149.43	175.46	39.82	14.85	26.34
$[Zn(HmpETSC)Cl_2]$	158.01	124.01	137.59	118.06	152.82	142.22	177.25	38.83	14.94	24.07
$[Ru(PPh_3)_2(mpETSC)_2]$	157.32	127.08	137.82	117.45	155.44	143.41	183.48	36.37	15.94	24.94
[Pd(mpETSC)Cl]	163.54	127.87	140.56	123.52	157.64	149.90	178.56	41.85	14.74	25.70
[Pt(mpETSC)Cl]	164.02	129.06	140.61	123.56	157.88	146.54	180.45	40.55	14.92	25.93

Table 5: Selected bond lengths and bond angles for $[VO_2(mpETSC)]$.

bond lengths (Å)		Bond angles (°)	
V(1)–O(1)	1.6145(12)	O(2)–V(1)–S(8)	96.73(5)
V(1)–O(2)	1.6356(12)	N(1)–V(1)–S(8)	151.43(4)
V(1)–N(1)	2.1333(14)	N(7)–V(1)–S(8)	76.48(4)
V(1)–N(7)	2.1651(13)	C(8)–S(8)–V(1)	100.39(6)
V(1)–S(8)	2.3800(5)	C(2)–N(1)–C(6)	118.72(14)
S(8)–C(8)	1.7472(17)	C(2)–N(1)–V(1)	125.52(11)
N(1)–C(2)	1.351(2)	C(6)–N(1)–V(1)	115.75(11)
N(1)–C(6)	1.361(2)	C(7)–N(7)–N(8)	116.94(13)
N(7)–C(7)	1.287(2)	C(7)–N(7)–V(1)	116.04(10)
N(7)–N(8)	1.3708(17)	N(8)–N(7)–V(1)	127.01(10)
N(8)–C(8)	1.322(2)	C(8)–N(8)–N(7)	111.43(13)
N(9)–C(8)	1.339(2)	C(8)–N(9)–C(9)	124.07(16)
N(9)–C(9)	1.454(2)	N(1)–C(2)–C(3)	120.41(16)
C(1)–C(2)	1.494(2)	N(1)–C(2)–C(1)	119.13(15)
C(2)–C(3)	1.398(2)	C(3)–C(2)–C(1)	120.45(15)
C(3)–C(4)	1.379(3)	C(4)–C(3)–C(2)	120.71(15)
C(4)–C(5)	1.390(2)	C(3)–C(4)–C(5)	118.81(16)
C(5)–C(6)	1.385(2)	C(6)–C(5)–C(4)	118.35(16)
C(6)–C(7)	1.451(2)	N(1)–C(6)–C(5)	122.94(16)
C(9)–C(10)	1.509(3)	N(1)–C(6)–C(7)	115.08(14)
		C(5)–C(6)–C(7)	121.98(15)
		N(7)–C(7)–C(6)	117.71(14)
		N(8)–C(8)–N(9)	118.62(15)
		N(8)–C(8)–S(8)	124.50(12)
		N(9)–C(8)–S(8)	116.87(13)
		N(9)–C(9)–C(10)	112.49(17)
		O(1)–V(1)–O(2)	107.64(7)
		O(1)–V(1)–N(1)	96.08(6)
		O(2)–V(1)–N(1)	101.30(6)
		O(1)–V(1)–N(7)	113.29(6)
		O(2)–V(1)–N(7)	139.07(6)
		N(1)–V(1)–N(7)	75.37(5)
		O(1)–V(1)–S(8)	99.35(5)

Table 6: Bond lengths [Å] and angles [°] related to the hydrogen bonding for $[VO_2(mpETSC)]$.

D-H	..A	d(D-H)	d(H..A)	d(D..A)	<DHA
N(9)–H(9)	O(2) no. 1	0.82(2)	2.30(2)	2.994(2)	144(2)

Symmetry transformations used to generate equivalent atoms: no. 1 $-x+1$, and $y-1/2$, $-z+3/2$.

to $^1A_{1g} \rightarrow {}^1B_{1g}$ and $^1A_{1g} \rightarrow {}^1E_g$ transitions, respectively, in square planar configurations [9–12].

The electronic spectrum of the diamagnetic $[Ru^{II}(PPh_3)_2(mpETSC)_2]$ shows bands at 532, 354, and 393 nm ($^1A_{1g} \rightarrow {}^1T_{1g}$, $^1A_{1g} \rightarrow {}^1T_{2g}$, and ligand (p-dp) transitions, respectively). These are attributed to a low-spin octahedral geometry around Ru(II) [10–12].

The electronic spectrum of the diamagnetic $[VO_2(mpETSC)]$ shows that two bands at 440 and 360 nm may be assigned to MLCT and n-π^* transitions, respectively [43].

3.5. X-Ray Crystallography. The structure of the complexes $[VO_2(mpETSC)]$ and [Pt(mpETSC)Cl], together with the atoms numbering scheme adopted is shown in Figures 2, 3, 4, and 5, respectively. The selected bond distances and bond angles of the complexes are listed in Tables 5, 6, 7, and 8, respectively. The complexes $[VO_2(mpETSC)]$ and [Pt(mpETSC)Cl] are crystallized in monoclinic lattice with space group symmetry P21/c and P21/n, respectively.

The X-ray crystal structure of $[VO_2(mpETSC)]$ shows that the vanadium(V) atom has a distorted square pyramidal environment in which $mpETSC^-$ is coordinated to the metal ion as a tridentate chelating agent binding *via* the deprotonated thiolat sulfur S(8), the azomethine nitrogen N(7), and pyridine nitrogen N(1) atoms, yielding two five-membered chelate rings (Figure 2) with bond distances

Table 7: Selected bond lengths and bond angles for the [Pt(mpETSC)Cl] complex.

bond lengths (Å)		Bond angles (°)	
Pt(1)–N(7)	1.979(5)	C(8)–S(1)–Pt1	95.02(11)
Pt(1)–N(1)	2.116(3)	C(2)–N(1)–C(6)	118.6(3)
Pt(1)–S(1)	2.2533(8)	C(2)–N(1)–Pt1	132.4(2)
Pt(1)–Cl(1)	2.3178(15)	C(6)–N(1)–Pt1	109.0(2)
S(1)–C(8)	1.757(3)	C(7)–N(7)–N(8)	121.8(5)
N(1)–C(2)	1.350(4)	C(7)–N(7)–Pt1	116.1(4)
N(1)–C(6)	1.370(5)	N(8)–N(7)–Pt1	121.9(3)
N(7)–C(7)	1.287(8)	C(8)–N(8)–N(7)	113.4(4)
N(7)–N(8)	1.365(6)	C(8)–N(9)–C(9)	127.1(3)
N(8)–C(8)	1.333(5)	N(1)–C(2)–C(3)	120.3(3)
N(9)–C(8)	1.331(4)	N(1)–C(2)–C(1)	119.7(3)
N(9)–C(9)	1.449(4)	C(3)–C(2)–C(1)	120.0(3)
C(1)–C(2)	1.494(4)	C(4)–C(3)–C(2)	121.1(3)
C(2)–C(3)	1.400(5)	C(3)–C(4)–C(5)	118.4(3)
C(3)–C(4)	1.370(5)	C(6)–C(5)–C(4)	119.1(3)
C(4)–C(5)	1.389(5)	N(1)–C(6)–C(5)	122.3(3)
C(5)–C(6)	1.381(5)	N(1)–C(6)–C(7)	116.5(4)
C(6)–C(7)	1.426(8)	C(5)–C(6)–C(7)	121.2(4)
C(9)–C(10)	1.491(5)	N(7)–C(7)–C(6)	117.7(6)
		N(9)–C(8)–N(8)	116.8(3)
		N(9)–C(8)–S(1)	118.8(3)
		N(8)–C(8)–S(1)	124.4(3)
		N(9)–C(9)–C(10)	113.1(3)
		N(7)–Pt1–N(1)	80.15(16)
		N(7)–Pt1–S(1)	85.25(14)
		N(1)–Pt1–S(1)	165.40(8)
		N(7)–Pt1–Cl1	174.13(12)
		N(1)–Pt1–Cl1	105.02(8)
		S(1)–Pt1–Cl1	89.57(4)

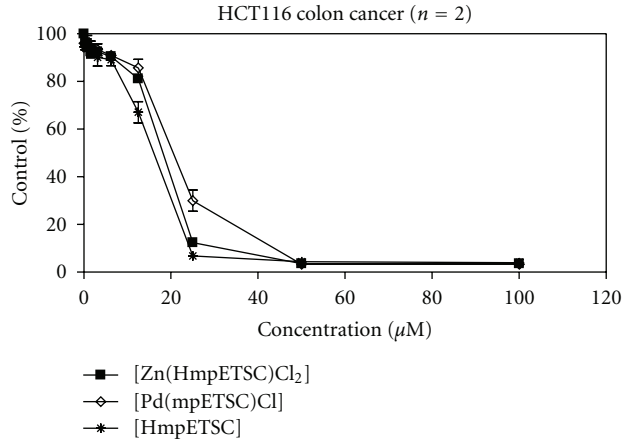

Figure 6: Antineoplastic activity in human colon carcinoma HCT116 cells by a growth inhibition SRB assay after 96-hour treatment of HmpETSC, [Zn(HmpETSC)Cl$_2$], and [Pd(mpETSC)Cl].

(V-N(1), 2.1333(14) Å, V-N(7), 2.1651(13) Å, and V-S(8), 2.3800(5) Å). The other two sites are occupied by oxo ligands

Table 8: Bond lengths (Å) and angles (°) related to the hydrogen bonding for [Pt(mpETSC)Cl].

D-H	..A	d(D-H)	d(H..A)	d(D..A)	<DHA
N(9)–H(9)	CL1 no. 1	0.88	2.62	3.372(3)	143.6

Symmetry transformations used to generate equivalent atoms: no. 1 $x + 1/2$, $-y + 3/2$, and $z + 1/2$.

Table 9: Antineoplastic activity in human colon tumor cell lines (HCT116) by growth inhibition SRB assay after 96-hour treatment.

Compound	HmpETSC	[Zn(HmpETSC)Cl$_2$]	[Pd(mpETSC)Cl]
IC$_{50}$, μM	14.59	16.96	20.65
SD	0.81	0.46	1.60

O(1) and O(2) in *cis*-configuration. The O(1) occupies the basal position with mpETSC$^-$ donor while the O(2) occupies the apical position (V-O(1), 1.6145(12) Å and V-O(2), 1.6356(12) Å) [42]. In the present complex [VO$_2$(mpETSC)], the bond distances C(8)-N(8), 1.322(2) Å and C(7)-N(7), 1.287(2) Å are not intermediate between single and double

bonds, but they are closer to double bonds. Also, the N(7)-N(8), 1.322(2) Å bond length is very close to a single bond (Table 5). Moreover, the C(8)-S(8) bond length in the complex (1.7472(7) Å) is intermediate between a C-S double bond (1.62 Å) and a C-S single bond (1.82 Å), indicating that this bond maintains a partial double-bond character [42]. The bond angles data, N(1)-V-N(7), 75.37(5) °; N(7)-V-S(8), 76.48(4)°, O(2)-V-S(8), 96.73(5)°, O(1)-V-O(2), 107.64(7)°, O(1)-V-N(1), 96.08(6)°, indicate that the complex has a distorted square pyramidal geometry, which may be attributed to the restricted bite angles of $mpETSC^-$ [44, 45]. The network structure is stabilized by the intermolecular hydrogen bonding interaction, N(9)H……O(2) bond (Table 6, Figure 3).

In case of [Pt(mpETSC)Cl], $mpETSC^-$ is also coordinated platinum(II) in the same tridentate manner, and chloride atom has taken up the fourth coordination site on Pt(II) in planar configuration (Figure 4). The bond lengths, Pt-N(1), 2.116(8) Å, Pt-N(7), 1.979(5) Å, Pt-S(1), 2.2533(8) Å, Pt-Cl(1), 2.3178(3) Å, in the complex are longer than those found in other reported square-planar platinum(II) complexes with N,S-donors [34–36, 42]. The data show that [Pt(mpETSC)Cl] has short N-N and long C-S bond lengths (Table 7) compared with other reported complexes. The bond angles of N(1)-Pt-S(1), 165.40(8)° and N(7)-Pt-Cl(1), 174.13(12)° are deviated substantially from that expected for a regular square-planar geometry. The monomer units of this complex are linked together into polymeric net chain through N(9)H….Cl intermolecular hydrogen bonds as shown in Table 8 and Figure 5 [46].

3.6. Antineoplastic Activity. HmpETSC, $[Zn(HmpETSC)Cl_2]$, and [Pd(mpETSC)Cl] were tested for their antineoplastic activity against the human colon tumor cell lines (HCT 116). The three compounds exhibited remarkable growth inhibitory activities with mean IC_{50} values of 14.59, 16.96, and 20.65 μM, respectively (Table 9 and Figure 6). 2-Formy and 2-acetylpyridine-N(4)-ethylthiosemicarbazones and their complexes $[M(f4Et)_2]$ and $[M(Ac4Et)_2]$ (M(II) = Pd, Pt, f4Et, Ac4Et = 2-formy and 2-acetylpyridine-N(4)-ethylthiosemicarbazone) have been tested in a panel of human colon, breast, and ovary tumor cell lines and were found to exhibit very remarkable growth inhibitory activities with mean IC_{50} values of 0.9–0.5 nM [47]. It is clear that the complexation of f4Et and Ac4Et in $[Pd(f4Et)_2]$, $[Pd(Ac4Et)_2]$, $[Pt(f4Et)_2]$, and $[Pt(Ac4Et)_2]$ modified their activities towards the tumor cells [47]. The complex $[Zn(HmpETSC)Cl_2]$ exhibits much better antineoplastic activity against HCT 116 compared to [Pd(mpETSC)Cl] which is more active than [Pt(mpETSC)Cl]. The substitution and modes of chelations of HmpETSC in the complexes $[Zn(HmpETSC)Cl_2]$ and [Pd(mpETSC)Cl] are different than both f4Et and Ac4Et in the reported Pd(II) and Pt(II) complexes [48]. As reported, *cis*-N_2 and *cis*-S_2 configuration in the complexes $[M(f4Et)_2]$ and $[M(Ac4Et)_2]$ (M(II) = Pd, Pt) display their significant antitumor activity [46, 49]. Also, in the $[Zn(HmpETSC)Cl_2]$, HmpETSC acts as a neutral bidentate chelating agent which is different than its behavior (mononegative tridentate) in [Pd(mpETSC)Cl]. Furthermore, the presence of the intermolecular hydrogen bonds in the later complex may reduce its antineoplastic activity [48].

4. Conclusion

The aim of this report is to study the structure and antineoplastic activity of 6-methylpyridine-2-carbaldehyde-N(4)-ethylthiosemicarbazone (HmpETSC) and its complexes with dioxovanadium(V), zinc(II), ruthenium(II), palladium(II), and platinum(II). The X-ray crystal structure of the complexes $[VO_2(mpETSC)]$ and [Pt(mpETSC)Cl] was reported. HmpETSC behaves as mononegative tridentate through the pyridine nitrogen, azomethine nitrogen and the deprotonated thiol sulfur atoms except in case of Zn(II) complex, it behaves as a neutral bidentate through azomethine nitrogen and thione sulfur atoms. HmpETSC and its Zn(II) and Pd(II) complexes show antineoplastic activity against the human colon tumor cell lines (HCT 116).

Acknowledgments

This research was supported by an NSERC (Canada) Discovery grant (ISB) and a scholarship from the Minsitry of Higher Education, Egypt (S.E.).

References

[1] V. B. Arion, M. A. Jakupec, M. Galanski, P. Unfried, and B. K. Keppler, "Synthesis, structure, spectroscopic and in vitro antitumour studies of a novel gallium(III) complex with 2-acetylpyridine ^{4}N-dimethylthiosemicarbazone," *Journal of Inorganic Biochemistry*, vol. 91, no. 1, pp. 298–305, 2002.

[2] C. C. García, B. N. Brousse, and M. J. Carlucci et al., "Inhibitory effect of thiosemicarbazone derivatives on Junin virus replication in vitro," *Antiviral Chemistry & Chemotherapy*, vol. 14, no. 2, pp. 99–105, 2003.

[3] W.-X. Hu, W. Zhou, C.-N. Xia, and X. Wen, "Synthesis and anticancer activity of thiosemicarbazones," *Bioorganic and Medicinal Chemistry Letters*, vol. 16, no. 8, pp. 2213–2218, 2006.

[4] E. M. Jouad, G. Larcher, and M. Allain et al., "Synthesis, structure and biological activity of nickel(II) complexes of 5-methyl 2-furfural thiosemicarbazone," *Journal of Inorganic Biochemistry*, vol. 86, no. 2-3, pp. 565–571, 2001.

[5] A. Gölcü, M. Dolaz, H. Demirelli, M. Diorak, and S. Serin, "Spectroscopic and analytic properties of new copper(II) complex of antiviral drug valacyclovir," *Transition Metal Chemistry*, vol. 31, no. 5, pp. 658–665, 2006.

[6] E. J. Blanz Jr. and F. A. French, "The carcinostatic activity of 5-hydroxy-2-formylpyridine thiosemicarbazone," *Cancer Research*, vol. 28, no. 12, pp. 2419–2422, 1968.

[7] D. Kovala-Demertzi, P. N. Yadav, J. Wiecek, S. Skoulika, T. Varadinova, and M. A. Demertzis, "Zinc(II) complexes derived from pyridine-2-carbaldehyde thiosemicarbazone and (1E)-1-pyridin-2-ylethan-1-one thiosemicarbazone. Synthesis, crystal structures and antiproliferative activity of zinc(II) complexes," *Journal of Inorganic Biochemistry*, vol. 100, no. 9, pp. 1558–1567, 2006.

[8] D. Kovala-Demertzi, M. A. Demertzis, and V. Varagi et al., "Antineoplastic and cytogenetic effects of platinum(II) and palladium(II) complexes with pyridine-2-carboxyaldehyde-thiosemicarbazone," *Chemotherapy*, vol. 44, no. 6, pp. 421–426, 1998.

[9] S. I. Mostafa, "Mixed ligand complexes with 2-piperidine-carboxylic acid as primary ligand and ethylene diamine, 2,2′-bipyridyl, 1,10-phenanthroline and 2(2′-pyridyl)quinoxaline as secondary ligands: preparation, characterization and biological activity," *Transition Metal Chemistry*, vol. 32, no. 6, pp. 769–775, 2007.

[10] S. I. Mostafa, "Synthesis, characterization and antineoplastic activity of 5-chloro-2,3-dihydroxypyridine transition metal complexes," *Journal of Coordination Chemistry*, vol. 61, no. 10, pp. 1553–1567, 2008.

[11] S. I. Mostafa and F. A. Badria, "Synthesis, spectroscopic, and anticancerous properties of mixed ligand palladium(II) and silver(I) complexes with 4,6-diamino-5-hydroxy-2- mercaptopyrimidine and 2,2′-bipyridyl," *Metal-Based Drugs*, vol. 2008, Article ID 723634, 7 pages, 2008.

[12] I. M. Gabr, H. A. El-Asmy, M. S. Emmam, and S. I. Mostafa, "Synthesis, characterization and anticancer activity of 3-aminopyrazine-2- carboxylic acid transition metal complexes," *Transition Metal Chemistry*, vol. 34, no. 4, pp. 409–418, 2009.

[13] D. X. West, S. L. Dietrich, I. Thientanavanich, C. A. Brown, and A. E. Liberta, "Copper(II) complexes of 6-methyl-2-formylpyridine ^{4}N-substituted thiosemicarbazones," *Transition Metal Chemistry*, vol. 19, no. 2, pp. 195–200, 1994.

[14] T. A. Stephenson and G. Wilkinson, "New complexes of ruthenium (II) and (III) with triphenylphosphine, triphenylarsine, trichlorostannate, pyridine and other ligands," *Journal of Inorganic and Nuclear Chemistry*, vol. 28, no. 4, pp. 945–956, 1966.

[15] P. Skehan, R. Storeng, and D. Scudiero et al., "New colorimetric cytotoxicity assay for anticancer-drug screening," *Journal of the National Cancer Institute*, vol. 82, no. 13, pp. 1107–1112, 1990.

[16] V. K. Sharma, S. Srivastava, and A. Srivastava, "Spectroscopic, thermal and biological studies on some trivalent ruthenium and rhodium NS chelating thiosemicarbazone complexes," *Bioinorganic Chemistry and Applications*, vol. 2007, Article ID 68374, 2007.

[17] M. A. Ali, N. E. H. Ibrahim, R. J. Butcher, J. P. Jasinski, J. M. Jasinski, and J. C. Bryan, "Synthesis and Characterization of some four-and five-coordinate copper(II)complexes of 6-methyl-2-formylpyridinethiosemicarbazone," *Polyhedron*, vol. 17, no. 11-12, pp. 1803–1809, 1998.

[18] O. E. Offiong and S. Martelli, "Stereochemistry and antitumour activity of platinum metal complexes of 2-acetylpyridine thiosemicarbazones," *Transition Metal Chemistry*, vol. 22, no. 3, pp. 263–269, 1997.

[19] S. I. Mostafa and M. M. Bekheit, "Synthesis and structure studies of complexes of some second row transition metals with 1-(phenylacetyl and phenoxyacetyl)-4-phenyl-3- thiosemicarbazide," *Chemical and Pharmaceutical Bulletin*, vol. 48, no. 2, pp. 266–271, 2000.

[20] Y. K. Bhoon, "Magnetic and EPR properties of Mn(II), Fe(III), Ni(II) and Cu(II) complexes of thiosemicarbazone of α-hydroxy-β-napthaldehyde," *Polyhedron*, vol. 2, no. 5, pp. 365–368, 1983.

[21] D. X. West and D. S. Galloway, "Transition metal ion complexes of thiosemicarbazones derived from 2-acetylpyridine. Part 3. The 3-hexamethyleneimine derivative," *Transition Metal Chemistry*, vol. 13, no. 6, pp. 410–414, 1988.

[22] S. Singh, N. Bharti, F. Naqvi, and A. Azam, "Synthesis, characterization and in vitro antiamoebic activity of 5-nitrothiophene-2-carboxaldehyde thiosemicarbazones and their Palladium (II) and Ruthenium (II) complexes," *European Journal of Medicinal Chemistry*, vol. 39, no. 5, pp. 459–465, 2004.

[23] S. Chandra and L. K. Gupta, "EPR, mass, IR, electronic, and magnetic studies on copper(II) complexes of semicarbazones and thiosemicarbazones," *Spectrochimica Acta—Part A*, vol. 61, no. 1-2, pp. 269–275, 2005.

[24] D. X. West, J. K. Swearingen, J. Valdés-Martínez, et al., "Spectral and structural studies of iron(III), cobalt(II,III) and nickel(II) complexes of 2-pyridineformamide N(4)-methylthiosemicarbazone," *Polyhedron*, vol. 18, no. 22, pp. 2919–2929, 1999.

[25] S. A. Elsayed, A. M. El-Hendawy, S. I. Mostafa, and I. S. Butler, " Transition metal complexes of 2-formylpyridine-ethiosemicarbazone (HFpyTSC) and X-Ray crystal structures of [Pd(FpyTSC)(PPh_3)]$PF_6$and [Pd(FpyTSC)(SCN)]," *Inorganica Chimica Acta*. In press.

[26] T. S. Lobana, R. Sharma, G. Bawa, and S. Khanna, "Bonding and structure trends of thiosemicarbazone derivatives of metals—an overview," *Coordination Chemistry Reviews*, vol. 253, no. 7-8, pp. 977–1055, 2009.

[27] D. X. West, A. E. Liberta, and S. B. Padhye et al., "Thiosemicarbazone complexes of copper(II): structural and biological studies," *Coordination Chemistry Reviews*, vol. 123, no. 1-2, pp. 49–71, 1993.

[28] S. Samanta, D. Ghosh, S. Mukhopadhyay, A. Endo, T. J. R. Weakley, and M. Chaudhury, "Oxovanadium(IV) and -(V) complexes of dithiocarbazate-based tridentate schiff base ligands: syntheses, structure, and photochemical reactivity of compounds involving imidazole derivatives as coligands," *Inorganic Chemistry*, vol. 42, no. 5, pp. 1508–1517, 2003.

[29] E. Kwiatkowski, G. Romanowski, W. Nowicki, M. Kwiatkowski, and K. Suwińska, "Dioxovanadium(V) Schiff base complexes of N-methyl-1,2-diaminoethane and 2-methyl-1,2-diaminopropane with aromatic O-hydroxyaldehydes and o-hydroxyketones: synthesis, characterisation, catalytic properties and structure," *Polyhedron*, vol. 22, no. 7, pp. 1009–1018, 2003.

[30] T. S. Lobana, G. Bawa, R. J. Butcher, B.-J. Liaw, and C. W. Liu, "Thiosemicarbazonates of ruthenium(II): crystal structures of [bis(diphenylphosphino)butane][bis(pyridine-2-carbaldehydethiosemicarbazonato)] ruthenium(II) and [bis(triphenylphosphine)] [bis(benzaldehydethiosemicarbazonato)] ruthenium(II)," *Polyhedron*, vol. 25, no. 15, pp. 2897–2903, 2006.

[31] K. R. Koch, "A multinuclear NMR study of platinum(II) complexes of N-Phenyl and N-(3-Allyl) Substituted 2-(2-Pyridinemethylene) hydrazine carbothioamides," *Journal of Coordination Chemistry*, vol. 22, no. 4, pp. 289–298, 1990.

[32] R. Pedrido, M. J. Romero, M. R. Bermejo, M. Martínez-Calvo, A. M. González-Noya, and G. Zaragoza, "Coordinative trends of a tridentate thiosemicarbazone ligand: synthesis, characterization, luminescence studies and desulfurization processes," *Dalton Transactions*, no. 39, pp. 8329–8340, 2009.

[33] W. Hernándeza, J. Paz, A. Vaisberg, E. Spodine, R. Richter, and L. Beyer, "Synthesis, characterization, and in vitro cytotoxic activities of benzaldehyde thiosemicarbazone derivatives and their palladium (II) and platinum (II) complexes against

various human tumor cell lines," *Bioinorganic Chemistry and Applications*, vol. 2008, Article ID 690952, 2008.

[34] D. Kovala-Demertzi, P. N. Yadav, J. Wiecek, S. Skoulika, T. Varadinova, and M. A. Demertzis, "Zinc(II) complexes derived from pyridine-2-carbaldehyde thiosemicarbazone and (1E)-1-pyridin-2-ylethan-1-one thiosemicarbazone. Synthesis, crystal structures and antiproliferative activity of zinc(II) complexes," *Journal of Inorganic Biochemistry*, vol. 100, no. 9, pp. 1558–1567, 2006.

[35] M. R. Bermejo, A. M. González-Noya, M. Martínez-Calvo, et al., "New neutral metal complexes from the 4-*N*-phenylthiosemicarbazone-2- pyridinecarboxaldehyde ligand - ^{113}Cd and ^{207}Pb NMR studies," *Zeitschrift für Anorganische und Allgemeine Chemie*, vol. 633, no. 11-12, pp. 1911–1918, 2007.

[36] R. Pedrido, A.M. González-Noya, M. J. Romero, et al., "Pentadentate thiosemicarbazones as versatile chelating systems. A comparative structural study of their metallic complexes," *Dalton Transactions*, no. 47, pp. 6776–6787, 2008.

[37] K. R. Koch, "Cationic and neutral bis(4-p-tolylthiosemicarbazido)platinum(II) complexes: a preparative as well as 1H and 195Pt NMR study of the question of cis/trans isomerism," *Inorganica Chimica Acta*, vol. 147, no. 2, pp. 227–232, 1988.

[38] A. Castineiras, D. X. West, H. Gebremedhin, and T. J. Romack, "Cobalt(III) complexes with 2-acetyl- and 2-formylpyridine 4N-methylthiosemicarbazones," *Inorganica Chimica Acta*, vol. 216, no. 1-2, pp. 229–236, 1994.

[39] W. P. Griffith and S. I. Mostafa, "Complexes of 3-hydroxypyridin-2-one and 1,2-dimethyl-3-hydroxypyridin-4-one with second and third row elements of groups 6, 7 and 8," *Polyhedron*, vol. 11, no. 23, pp. 2997–3005, 1992.

[40] I. C. Mendes, J. P. Moreira, N. L. Speziali, A. S. Mangrich, J. A. Takahashi, and H. Beraldo, "N(4)-tolyl-2-benzoylpyridine thiosemicarbazones and their copper(II) complexes with significant antifungal activity. Crystal structure of N(4)-para-tolyl-2-benzoylpyridine thiosemicarbazone," *Journal of the Brazilian Chemical Society*, vol. 17, no. 8, pp. 1571–1577, 2006.

[41] I. C. Mendes, J. P. Moreira, A. S. Mangrich, S. P. Balena, B. L. Rodrigues, and H. Beraldo, "Coordination to copper(II) strongly enhances the in vitro antimicrobial activity of pyridine-derived N(4)-tolyl thiosemicarbazones," *Polyhedron*, vol. 26, no. 13, pp. 3263–3270, 2007.

[42] M. A. Ali, A. H. Mirza, R. J. Butcher, M. T. H. Tarafder, T. B. Keat, and A. M. Ali, "Biological activity of palladium(II) and platinum(II) complexes of the acetone Schiff bases of *S*-methyl- and *S*-benzyldithiocarbazate and the X-ray crystal structure of the [Pd(asme)2] (asme=anionic form of the acetone Schiff base of S-methyldithiocarbazate) complex," *Journal of Inorganic Biochemistry*, vol. 92, no. 3-4, pp. 141–148, 2002.

[43] I. C. Mendes, L. M. Botion, A. V. M. Ferreira, E. E. Castellano, and H. Beraldo, "Vanadium complexes with 2-pyridineformamide thiosemicarbazones: in vitro studies of insulin-like activity," *Inorganica Chimica Acta*, vol. 362, no. 2, pp. 414–420, 2009.

[44] P. I. S. Maia, F. R. Pavan, and C. Q. F. Leite et al., "Vanadium complexes with thiosemicarbazones: synthesis, characterization, crystal structures and anti-Mycobacterium tuberculosis activity," *Polyhedron*, vol. 28, no. 2, pp. 398–406, 2009.

[45] A. Sreekanth, S. Sivakumar, and M. R. P. Kurup, "Structural studies of six and four coordinate zinc(II), nickel(II) and dioxovanadium(V) complexes with thiosemicarbazones," *Journal of Molecular Structure*, vol. 655, no. 1, pp. 47–58, 2003.

[46] D. Kovala-Demertzi, M. A. Demertzis, J. R. Miller, C. Papadopoulou, C. Dodorou, and G. Filousis, "Platinum(II) complexes with 2-acetyl pyridine thiosemicarbazone: synthesis, crystal structure, spectral properties, antimicrobial and antitumour activity," *Journal of Inorganic Biochemistry*, vol. 86, no. 2-3, pp. 555–563, 2001.

[47] D. Kovala-Demertzi, A. Boccarelli, M. A. Demertzis, and M. Coluccia, "In vitro antitumor activity of 2-acetyl pyridine 4N-ethyl thiosemicarbazone and its platinum(II) and palladium(II) complexes," *Chemotherapy*, vol. 53, no. 2, pp. 148–152, 2007.

[48] A. I. Matesanz and P. Souza, "Palladium and platinum 3,5-diacetyl-1,2,4-triazol bis(thiosemicarbazones): chemistry, cytotoxic activity and structure-activity relationships," *Journal of Inorganic Biochemistry*, vol. 101, no. 2, pp. 245–253, 2007.

[49] K. I. Goldberg, J. Valdes-Martínez, G. Espinosa-Pérez, L. J. Ackerman, and D. X. West, "Palladium(II) and platinum(II) complexes of 6-methyl-2-acetylpyridine 3-hexamethyleneiminylthiosemicarbazones: a structural and spectral study," *Polyhedron*, vol. 18, no. 8-9, pp. 1177–1182, 1999.